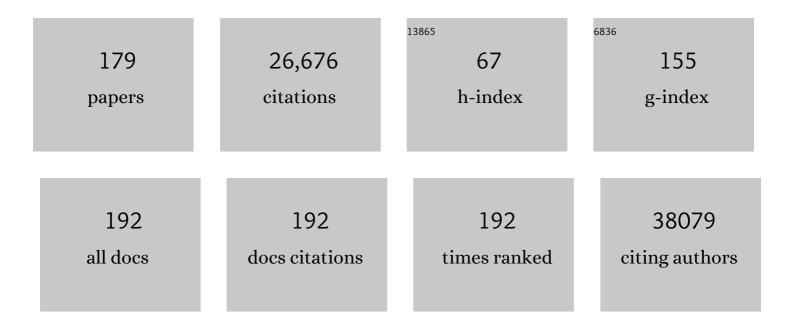


List of Publications by Year in descending order

Source: https://exaly.com/author-pdf/2996869/publications.pdf Version: 2024-02-01



Ηλο λλμ

#	Article	IF	CITATIONS
1	LIN28 coordinately promotes nucleolar/ribosomal functions and represses the 2C-like transcriptional program in pluripotent stem cells. Protein and Cell, 2022, 13, 490-512.	11.0	28
2	Neuronal Yin Yang1 in the prefrontal cortex regulates transcriptional and behavioral responses to chronic stress in mice. Nature Communications, 2022, 13, 55.	12.8	14
3	A comprehensive comparison of supervised and unsupervised methods for cell type identification in single-cell RNA-seq. Briefings in Bioinformatics, 2022, 23, .	6.5	22
4	Detection of Newly Secreted Antibodies Predicts Nonrecurrence in Primary Clostridioides difficile Infection. Journal of Clinical Microbiology, 2022, 60, jcm0220121.	3.9	5
5	EDClust: an EM–MM hybrid method for cell clustering in multiple-subject single-cell RNA sequencing. Bioinformatics, 2022, 38, 2692-2699.	4.1	4
6	Differential Methylation Analysis for Bisulfite Sequencing (BS-Seq) Data. Methods in Molecular Biology, 2022, 2432, 211-226.	0.9	0
7	Altered hydroxymethylome in the substantia nigra of Parkinson's disease. Human Molecular Genetics, 2022, 31, 3494-3503.	2.9	7
8	Complete deconvolution of DNA methylation signals from complex tissues: a geometric approach. Bioinformatics, 2021, 37, 1052-1059.	4.1	2
9	Downregulation of SOCS gene expression can inhibit the formation of acute and persistent BDV infections. Scandinavian Journal of Immunology, 2021, 93, e12974.	2.7	4
10	Predictive modeling of single-cell DNA methylome data enhances integration with transcriptome data. Genome Research, 2021, 31, 101-109.	5.5	12
11	Novel immunoassay for diagnosis of ongoing Clostridioides difficile infections using serum and medium enriched for newly synthesized antibodies (MENSA). Journal of Immunological Methods, 2021, 492, 112932.	1.4	7
12	The long noncoding RNA IncCIRBIL disrupts the nuclear translocation of Bclaf1 alleviating cardiac ischemia–reperfusion injury. Nature Communications, 2021, 12, 522.	12.8	32
13	Accurate feature selection improves single-cell RNA-seq cell clustering. Briefings in Bioinformatics, 2021, 22, .	6.5	31
14	Pneumonia scoring systems for severe COVID-19: which one is better. Virology Journal, 2021, 18, 33.	3.4	15
15	Penalized Latent Dirichlet Allocation Model in Single-Cell RNA Sequencing. Statistics in Biosciences, 2021, 13, 543-562.	1.2	5
16	Downregulation of <i>TOP2</i> modulates neurodegeneration caused by GGGGCC expanded repeats. Human Molecular Genetics, 2021, 30, 893-901.	2.9	4
17	Detecting m6A methylation regions from Methylated RNA Immunoprecipitation Sequencing. Bioinformatics, 2021, 37, 2818-2824.	4.1	10
18	Non-linear Normalization for Non-UMI Single Cell RNA-Seq. Frontiers in Genetics, 2021, 12, 612670.	2.3	3

#	Article	IF	CITATIONS
19	Dual effects of N6-methyladenosine on cancer progression and immunotherapy. Molecular Therapy - Nucleic Acids, 2021, 24, 25-39.	5.1	20
20	A human forebrain organoid model of fragile X syndrome exhibits altered neurogenesis and highlights new treatment strategies. Nature Neuroscience, 2021, 24, 1377-1391.	14.8	80
21	Evaluation of some aspects in supervised cell type identification for single-cell RNA-seq: classifier, feature selection, and reference construction. Genome Biology, 2021, 22, 264.	8.8	21
22	N6-methyladenosine dynamics in neurodevelopment and aging, and its potential role in Alzheimer's disease. Genome Biology, 2021, 22, 17.	8.8	131
23	Bisulfite-Free Sequencing of 5-Hydroxymethylcytosine with APOBEC-Coupled Epigenetic Sequencing (ACE-Seq). Methods in Molecular Biology, 2021, 2198, 349-367.	0.9	7
24	Influence of painless delivery on the maternal and neonatal outcomes under the guidance of new concept of labor American Journal of Translational Research (discontinued), 2021, 13, 12973-12979.	0.0	0
25	A comprehensive review of computational prediction of genome-wide features. Briefings in Bioinformatics, 2020, 21, 120-134.	6.5	12
26	Age-related DNA hydroxymethylation is enriched for gene expression and immune system processes in human peripheral blood. Epigenetics, 2020, 15, 294-306.	2.7	8
27	Ethnicity-specific and overlapping alterations of brain hydroxymethylome in Alzheimer's disease. Human Molecular Genetics, 2020, 29, 149-158.	2.9	11
28	Pan-cancer analysis of differential DNA methylation patterns. BMC Medical Genomics, 2020, 13, 154.	1.5	7
29	Near-infrared fluorescence imaging-guided focused ultrasound-mediated therapy against Rheumatoid Arthritis by MTX-ICG-loaded iRGD-modified echogenic liposomes. Theranostics, 2020, 10, 10092-10105.	10.0	32
30	Massively parallel and time-resolved RNA sequencing in single cells with scNT-seq. Nature Methods, 2020, 17, 991-1001.	19.0	103
31	Palliative Radiofrequency Ablation Accelerates the Residual Tumor Progression Through Increasing Tumor-Infiltrating MDSCs and Reducing T-Cell-Mediated Anti-Tumor Immune Responses in Animal Model. Frontiers in Oncology, 2020, 10, 1308.	2.8	17
32	Accounting for cell type hierarchy in evaluating single cell RNA-seq clustering. Genome Biology, 2020, 21, 123.	8.8	20
33	Single-cell transcriptomic analysis of adult mouse pituitary reveals sexual dimorphism and physiologic demand-induced cellular plasticity. Protein and Cell, 2020, 11, 565-583.	11.0	55
34	Photobiomodulation with 630-nm LED radiation inhibits the proliferation of human synoviocyte MH7A cells possibly via TRPV4/PI3K/AKT/mTOR signaling pathway. Lasers in Medical Science, 2020, 35, 1927-1936.	2.1	17
35	Robust partial reference-free cell composition estimation from tissue expression. Bioinformatics, 2020, 36, 3431-3438.	4.1	12
36	Sliced Human Cortical Organoids for Modeling Distinct Cortical Layer Formation. Cell Stem Cell, 2020, 26, 766-781.e9.	11.1	268

#	Article	lF	CITATIONS
37	Simulation, power evaluation and sample size recommendation for single-cell RNA-seq. Bioinformatics, 2020, 36, 4860-4868.	4.1	14
38	Tet2-mediated epigenetic drive for astrocyte differentiation from embryonic neural stem cells. Cell Death Discovery, 2020, 6, 30.	4.7	7
39	TOAST: improving reference-free cell composition estimation by cross-cell type differential analysis. Genome Biology, 2019, 20, 190.	8.8	42
40	Glioblastoma extracellular vesicles induce the tumour-promoting transformation of neural stem cells. Cancer Letters, 2019, 466, 1-12.	7.2	34
41	The molecular mechanism study of insulin on proliferation and differentiation of osteoblasts under high glucose conditions. Cell Biochemistry and Function, 2019, 37, 385-394.	2.9	9
42	The molecular mechanism study of insulin in promoting wound healing under highâ€glucose conditions. Journal of Cellular Biochemistry, 2019, 120, 16244-16253.	2.6	6
43	Dissecting differential signals in high-throughput data from complex tissues. Bioinformatics, 2019, 35, 3898-3905.	4.1	35
44	miR-29c-3p regulates DNMT3B and LATS1 methylation to inhibit tumor progression in hepatocellular carcinoma. Cell Death and Disease, 2019, 10, 48.	6.3	72
45	Differential methylation analysis for bisulfite sequencing using DSS. Quantitative Biology, 2019, 7, 327-334.	0.5	21
46	Disease prediction by cell-free DNA methylation. Briefings in Bioinformatics, 2019, 20, 585-597.	6.5	35
47	Two-phase differential expression analysis for single cell RNA-seq. Bioinformatics, 2018, 34, 3340-3348.	4.1	34
48	Rescue of Fragile X Syndrome Neurons by DNA Methylation Editing of the FMR1 Gene. Cell, 2018, 172, 979-992.e6.	28.9	351
49	Epitranscriptomic m6A Regulation of Axon Regeneration in the Adult Mammalian Nervous System. Neuron, 2018, 97, 313-325.e6.	8.1	292
50	The nuclear matrix protein HNRNPU maintains 3D genome architecture globally in mouse hepatocytes. Genome Research, 2018, 28, 192-202.	5.5	91
51	InfiniumPurify: An R package for estimating and accounting for tumor purity in cancer methylation research. Genes and Diseases, 2018, 5, 43-45.	3.4	48
52	A High Throughput Whole Blood Assay for Analysis of Multiple Antigen-Specific T Cell Responses in Human <i>Mycobacterium tuberculosis</i> Infection. Journal of Immunology, 2018, 200, 3008-3019.	0.8	11
53	Ten-Eleven Translocation Proteins Modulate the Response to Environmental Stress in Mice. Cell Reports, 2018, 25, 3194-3203.e4.	6.4	46
54	Nondestructive, base-resolution sequencing of 5-hydroxymethylcytosine using a DNA deaminase. Nature Biotechnology, 2018, 36, 1083-1090.	17.5	154

HAO WU

#	Article	IF	CITATIONS
55	5-Hydroxymethylcytosine alterations in the human postmortem brains of autism spectrum disorder. Human Molecular Genetics, 2018, 27, 2955-2964.	2.9	28
56	Active N6-Methyladenine Demethylation by DMAD Regulates Gene Expression by Coordinating with Polycomb Protein in Neurons. Molecular Cell, 2018, 71, 848-857.e6.	9.7	71
57	Fragile X mental retardation protein modulates the stability of its m6A-marked messenger RNA targets. Human Molecular Genetics, 2018, 27, 3936-3950.	2.9	129
58	A genomeâ€wide profiling of brain DNA hydroxymethylation in Alzheimer's disease. Alzheimer's and Dementia, 2017, 13, 674-688.	0.8	83
59	Epigenomic reprogramming during pancreatic cancer progression links anabolic glucose metabolism to distant metastasis. Nature Genetics, 2017, 49, 367-376.	21.4	365
60	PLEMT: A Novel Pseudolikelihood-Based EM Test for Homogeneity in Generalized Exponential Tilt Mixture Models. Journal of the American Statistical Association, 2017, 112, 1393-1404.	3.1	7
61	Open-ringed structure of the Cdt1–Mcm2–7 complex as a precursor of the MCM double hexamer. Nature Structural and Molecular Biology, 2017, 24, 300-308.	8.2	87
62	Fat mass and obesity-associated (FTO) protein regulates adult neurogenesis. Human Molecular Genetics, 2017, 26, 2398-2411.	2.9	221
63	Accounting for tumor purity improves cancer subtype classification from DNA methylation data. Bioinformatics, 2017, 33, 2651-2657.	4.1	32
64	Differential gene network analysis from single cell RNA-seq. Journal of Genetics and Genomics, 2017, 44, 331-334.	3.9	7
65	DNA N6-methyladenine is dynamically regulated in the mouse brain following environmental stress. Nature Communications, 2017, 8, 1122.	12.8	182
66	Integrating Next-Generation Genomic Sequencing and Mass Spectrometry To Estimate Allele-Specific Protein Abundance in Human Brain. Journal of Proteome Research, 2017, 16, 3336-3347.	3.7	48
67	Zika virus directly infects peripheral neurons and induces cell death. Nature Neuroscience, 2017, 20, 1209-1212.	14.8	85
68	Hypoxiaâ€inducible protein 2 Hig2/Hilpda mediates neutral lipid accumulation in macrophages and contributes to atherosclerosis in apolipoprotein E–deficient mice. FASEB Journal, 2017, 31, 4971-4984.	0.5	50
69	Dissecting Cell-Type Composition and Activity-Dependent Transcriptional State in Mammalian Brains by Massively Parallel Single-Nucleus RNA-Seq. Molecular Cell, 2017, 68, 1006-1015.e7.	9.7	143
70	Estimating and accounting for tumor purity in the analysis of DNA methylation data from cancer studies. Genome Biology, 2017, 18, 17.	8.8	112
71	Ten-eleven translocation 2 interacts with forkhead box O3 and regulates adult neurogenesis. Nature Communications, 2017, 8, 15903.	12.8	82
72	Effects of slow and regular breathing exercise on cardiopulmonary coupling and blood pressure. Medical and Biological Engineering and Computing, 2017, 55, 327-341.	2.8	26

#	Article	IF	CITATIONS
73	ROC Curve Analysis in the Presence of Imperfect Reference Standards. Statistics in Biosciences, 2017, 9, 91-104.	1.2	13
74	Tumor purity and differential methylation in cancer epigenomics. Briefings in Functional Genomics, 2016, 15, elw016.	2.7	13
75	Brain-Region-Specific Organoids Using Mini-bioreactors for Modeling ZIKV Exposure. Cell, 2016, 165, 1238-1254.	28.9	1,680
76	A robust approach for ECG-based analysis of cardiopulmonary coupling. Medical Engineering and Physics, 2016, 38, 671-678.	1.7	10
77	Base-resolution profiling of active DNA demethylation using MAB-seq and caMAB-seq. Nature Protocols, 2016, 11, 1081-1100.	12.0	30
78	Molecular signatures associated with ZIKV exposure in human cortical neural progenitors. Nucleic Acids Research, 2016, 44, 8610-8620.	14.5	155
79	Negative Allosteric Modulation of mGluR5 Partially Corrects Pathophysiology in a Mouse Model of Rett Syndrome. Journal of Neuroscience, 2016, 36, 11946-11958.	3.6	41
80	Editing DNA Methylation in the Mammalian Genome. Cell, 2016, 167, 233-247.e17.	28.9	932
81	Endothelin-1 supports clonal derivation and expansion of cardiovascular progenitors derived from human embryonic stem cells. Nature Communications, 2016, 7, 10774.	12.8	21
82	NanoStringDiff: a novel statistical method for differential expression analysis based on NanoString nCounter data. Nucleic Acids Research, 2016, 44, gkw677.	14.5	100
83	Inhibition of ileal bile acid uptake protects against nonalcoholic fatty liver disease in high-fat diet–fed mice. Science Translational Medicine, 2016, 8, 357ra122.	12.4	160
84	Lin28A Binds Active Promoters and Recruits Tet1 to Regulate Gene Expression. Molecular Cell, 2016, 61, 153-160.	9.7	74
85	Statistical Challenges in Analyzing Methylation and Long-Range Chromosomal Interaction Data. Statistics in Biosciences, 2016, 8, 284-309.	1.2	9
86	Experimental Design and Power Calculation for RNA-seq Experiments. Methods in Molecular Biology, 2016, 1418, 379-390.	0.9	13
87	Measuring the spatial correlations of protein binding sites. Bioinformatics, 2016, 32, 1766-1772.	4.1	2
88	Differential methylation analysis for BS-seq data under general experimental design. Bioinformatics, 2016, 32, 1446-1453.	4.1	336
89	High glucose microenvironments inhibit the proliferation and migration of bone mesenchymal stem cells by activating GSK3β. Journal of Bone and Mineral Metabolism, 2016, 34, 140-150.	2.7	41
90	Abstract 607: Modulating VEGFR3 Signaling by Epsins Regulates Lymphatic Dysfuntion in Diabetes. Arteriosclerosis, Thrombosis, and Vascular Biology, 2016, 36, .	2.4	0

HAO WU

#	Article	IF	CITATIONS
91	Network-based survival-associated module biomarker and its crosstalk with cell death genes in ovarian cancer. Scientific Reports, 2015, 5, 11566.	3.3	36
92	Local false discovery rate estimation using feature reliability in LC/MS metabolomics data. Scientific Reports, 2015, 5, 17221.	3.3	24
93	MacroH2A1 associates with nuclear lamina and maintains chromatin architecture in mouse liver cells. Scientific Reports, 2015, 5, 17186.	3.3	44
94	Computer Simulation, Bioinformatics, and Statistical Analysis of Cancer Data and Processes. Cancer Informatics, 2015, 14s2, CIN.S32525.	1.9	0
95	Base-resolution methylation patterns accurately predict transcription factor bindings in vivo. Nucleic Acids Research, 2015, 43, 2757-2766.	14.5	46
96	SynBioLGDB: a resource for experimentally validated logic gates in synthetic biology. Scientific Reports, 2015, 5, 8090.	3.3	13
97	ViRBase: a resource for virus–host ncRNA-associated interactions. Nucleic Acids Research, 2015, 43, D578-D582.	14.5	81
98	Long-Lived Plasma Cells Are Contained within the CD19â^'CD38hiCD138+ Subset in Human Bone Marrow. Immunity, 2015, 43, 132-145.	14.3	415
99	Plasmodium knowlesi gene expression differs in ex vivo compared to in vitro blood-stage cultures. Malaria Journal, 2015, 14, 110.	2.3	31
100	A novel statistical method for quantitative comparison of multiple ChIP-seq datasets. Bioinformatics, 2015, 31, 1889-1896.	4.1	48
101	Predicting tumor purity from methylation microarray data. Bioinformatics, 2015, 31, 3401-3405.	4.1	50
102	Charting oxidized methylcytosines at base resolution. Nature Structural and Molecular Biology, 2015, 22, 656-661.	8.2	62
103	Detection of differentially methylated regions from whole-genome bisulfite sequencing data without replicates. Nucleic Acids Research, 2015, 43, gkv715.	14.5	203
104	PROPER: comprehensive power evaluation for differential expression using RNA-seq. Bioinformatics, 2015, 31, 233-241.	4.1	80
105	High-fat diet induced insulin resistance in pregnant rats through pancreatic pax6 signaling pathway. International Journal of Clinical and Experimental Pathology, 2015, 8, 5196-202.	0.5	17
106	PolyaPeak: Detecting Transcription Factor Binding Sites from ChIP-seq Using Peak Shape Information. PLoS ONE, 2014, 9, e89694.	2.5	13
107	Incorporating feature reliability in false discovery rateestimation improves statistical power to detect differentially expressed features. , 2014, , .		0
108	N-cadherin prevents the premature differentiation of anterior heart field progenitors in the pharyngeal mesodermal microenvironment. Cell Research, 2014, 24, 1420-1432.	12.0	35

#	Article	IF	CITATIONS
109	A Bayesian hierarchical model to detect differentially methylated loci from single nucleotide resolution sequencing data. Nucleic Acids Research, 2014, 42, e69-e69.	14.5	405
110	Genome-wide alteration of 5-hydroxymethylcytosine in a mouse model of fragile X-associated tremor/ataxia syndrome. Human Molecular Genetics, 2014, 23, 1095-1107.	2.9	52
111	Modeling Parkinson's disease in monkeys for translational studies, a critical analysis. Experimental Neurology, 2014, 256, 133-143.	4.1	62
112	Cellular Resolution Maps of X Chromosome Inactivation: Implications for Neural Development, Function, and Disease. Neuron, 2014, 81, 103-119.	8.1	179
113	Reversing DNA Methylation: Mechanisms, Genomics, and Biological Functions. Cell, 2014, 156, 45-68.	28.9	914
114	Single-base resolution analysis of active DNA demethylation using methylase-assisted bisulfite sequencing. Nature Biotechnology, 2014, 32, 1231-1240.	17.5	139
115	Deletion of Atbf1/Zfhx3 In Mouse Prostate Causes Neoplastic Lesions, Likely by Attenuation of Membrane and Secretory Proteins and Multiple Signaling Pathways. Neoplasia, 2014, 16, 377-389.	5.3	31
116	HMMR Maintains the Stemness and Tumorigenicity of Glioblastoma Stem-like Cells. Cancer Research, 2014, 74, 3168-3179.	0.9	101
117	Flat Mount Imaging of Mouse Skin and Its Application to the Analysis of Hair Follicle Patterning and Sensory Axon Morphology. Journal of Visualized Experiments, 2014, , e51749.	0.3	17
118	Complete morphologies of basal forebrain cholinergic neurons in the mouse. ELife, 2014, 3, e02444.	6.0	133
119	Cardiac regenerative medicine 2.0. Nature Biotechnology, 2013, 31, 209-211.	17.5	3
120	U1 small nuclear ribonucleoprotein complex and RNA splicing alterations in Alzheimer's disease. Proceedings of the National Academy of Sciences of the United States of America, 2013, 110, 16562-16567.	7.1	268
121	Cell-Cycle Control of Developmentally Regulated Transcription Factors Accounts for Heterogeneity in Human Pluripotent Cells. Stem Cell Reports, 2013, 1, 532-544.	4.8	129
122	Kdm2b maintains murine embryonic stem cell status by recruiting PRC1 complex to CpG islands of developmental genes. Nature Cell Biology, 2013, 15, 373-384.	10.3	292
123	A new shrinkage estimator for dispersion improves differential expression detection in RNA-seq data. Biostatistics, 2013, 14, 232-243.	1.5	210
124	Genome-wide Profiling of 5-Formylcytosine Reveals Its Roles in Epigenetic Priming. Cell, 2013, 153, 678-691.	28.9	502
125	Genome-wide Analysis Reveals TET- and TDG-Dependent 5-Methylcytosine Oxidation Dynamics. Cell, 2013, 153, 692-706.	28.9	440
126	Subtelomeric hotspots of aberrant 5-hydroxymethylcytosine-mediated epigenetic modifications during reprogramming to pluripotency. Nature Cell Biology, 2013, 15, 700-711.	10.3	87

HAO WU

#	Article	IF	CITATIONS
127	Exploring the Cooccurrence Patterns of Multiple Sets of Genomic Intervals. BioMed Research International, 2013, 2013, 1-7.	1.9	2
128	Regulation and function of mammalian DNA methylation patterns: a genomic perspective. Briefings in Functional Genomics, 2012, 11, 240-250.	2.7	33
129	Highly efficient derivation of ventricular cardiomyocytes from induced pluripotent stem cells with a distinct epigenetic signature. Cell Research, 2012, 22, 142-154.	12.0	77
130	Early Embryos Reprogram DNA Methylation in Two Steps. Cell Stem Cell, 2012, 10, 487-489.	11.1	11
131	Fragile X premutation RNA is sufficient to cause primary ovarian insufficiency in mice. Human Molecular Genetics, 2012, 21, 5039-5047.	2.9	78
132	Genome-wide DNA hydroxymethylation changes are associated with neurodevelopmental genes in the developing human cerebellum. Human Molecular Genetics, 2012, 21, 5500-5510.	2.9	157
133	Euchromatin islands in large heterochromatin domains are enriched for CTCF binding and differentially DNA-methylated regions. BMC Genomics, 2012, 13, 566.	2.8	40
134	Statistics for Next Generation Sequencing – Meeting Report. Frontiers in Genetics, 2012, 3, 128.	2.3	0
135	Morphologic diversity of cutaneous sensory afferents revealed by genetically directed sparse labeling. ELife, 2012, 1, e00181.	6.0	56
136	JAMIE: A Software Tool for Jointly Analyzing Multiple ChIP-chip Experiments. Methods in Molecular Biology, 2012, 802, 363-375.	0.9	1
137	Genome-wide analysis of 5-hydroxymethylcytosine distribution reveals its dual function in transcriptional regulation in mouse embryonic stem cells. Genes and Development, 2011, 25, 679-684.	5.9	488
138	Mechanisms and functions of Tet protein-mediated 5-methylcytosine oxidation. Genes and Development, 2011, 25, 2436-2452.	5.9	565
139	Tet1 and 5-hydroxymethylation. Cell Cycle, 2011, 10, 2428-2436.	2.6	121
140	Increased methylation variation in epigenetic domains across cancer types. Nature Genetics, 2011, 43, 768-775.	21.4	968
141	5-hmC–mediated epigenetic dynamics during postnatal neurodevelopment and aging. Nature Neuroscience, 2011, 14, 1607-1616.	14.8	746
142	Genome-scale epigenetic reprogramming during epithelial-to-mesenchymal transition. Nature Structural and Molecular Biology, 2011, 18, 867-874.	8.2	340
143	Dual functions of Tet1 in transcriptional regulation in mouse embryonic stem cells. Nature, 2011, 473, 389-393.	27.8	581
144	Deletion of Astroglial Dicer Causes Non-Cell-Autonomous Neuronal Dysfunction and Degeneration. Journal of Neuroscience, 2011, 31, 8306-8319.	3.6	154

#	Article	IF	CITATIONS
145	Reply to "Reassessing the abundance of H3K9me2 chromatin domains in embryonic stem cells― Nature Genetics, 2010, 42, 5-6.	21.4	32
146	Intensity normalization improves color calling in SOLiD sequencing. Nature Methods, 2010, 7, 336-337.	19.0	31
147	JAMIE: joint analysis of multiple ChIP-chip experiments. Bioinformatics, 2010, 26, 1864-1870.	4.1	12
148	Building the Quality Control System for Medical Equipments in Hospital. , 2010, , .		5
149	Genome-wide analysis reveals methyl-CpG–binding protein 2–dependent regulation of microRNAs in a mouse model of Rett syndrome. Proceedings of the National Academy of Sciences of the United States of America, 2010, 107, 18161-18166.	7.1	164
150	Redefining CpG islands using hidden Markov models. Biostatistics, 2010, 11, 499-514.	1.5	151
151	A smartphone based respiratory biofeedback system. , 2010, , .		18
152	Dnmt3a-Dependent Nonpromoter DNA Methylation Facilitates Transcription of Neurogenic Genes. Science, 2010, 329, 444-448.	12.6	544
153	Measurement Data Correction for Emission Tomography. , 2009, , .		0
154	A Prototype of Wearable Respiration Biofeedback Platform and Its Preliminary Evaluation on Cardiovascular Variability. , 2009, , .		13
155	Deciphering Rett Syndrome with Mouse Genetics, Epigenomics, and Human Neurons. International Review of Neurobiology, 2009, 89, 147-160.	2.0	9
156	Phosphorylation of MeCP2 at Serine 80 regulates its chromatin association and neurological function. Proceedings of the National Academy of Sciences of the United States of America, 2009, 106, 4882-4887.	7.1	200
157	Reversing DNA Methylation: New Insights from Neuronal Activity–Induced Gadd45b in Adult Neurogenesis. Science Signaling, 2009, 2, pe17.	3.6	34
158	Ago2 Immunoprecipitation Identifies Predicted MicroRNAs in Human Embryonic Stem Cells and Neural Precursors. PLoS ONE, 2009, 4, e7192.	2.5	103
159	A species-generalized probabilistic model-based definition of CpG islands. Mammalian Genome, 2009, 20, 674-80.	2.2	52
160	Large histone H3 lysine 9 dimethylated chromatin blocks distinguish differentiated from embryonic stem cells. Nature Genetics, 2009, 41, 246-250.	21.4	540
161	Copy Number Variant Analysis of Human Embryonic Stem Cells. Stem Cells, 2008, 26, 1484-1489.	3.2	50
162	Crystal structure of human coactosin-like protein at 1.9 Ã resolution. Protein Science, 2008, 13, 2845-2851.	7.6	9

#	Article	IF	CITATIONS
163	CD133 ⁺ neural stem cells in the ependyma of mammalian postnatal forebrain. Proceedings of the National Academy of Sciences of the United States of America, 2008, 105, 1026-1031.	7.1	300
164	Comprehensive high-throughput arrays for relative methylation (CHARM). Genome Research, 2008, 18, 780-790.	5.5	379
165	Overlapping euchromatin/heterochromatin- associated marks are enriched in imprinted gene regions and predict allele-specific modification. Genome Research, 2008, 18, 1806-1813.	5.5	29
166	Integrative genomic and functional analyses reveal neuronal subtype differentiation bias in human embryonic stem cell lines. Proceedings of the National Academy of Sciences of the United States of America, 2007, 104, 13821-13826.	7.1	131
167	Histone modifications around individual BDNF gene promoters in prefrontal cortex are associated with extinction of conditioned fear. Learning and Memory, 2007, 14, 268-276.	1.3	491
168	R/qtlbim: QTL with Bayesian Interval Mapping in experimental crosses. Bioinformatics, 2007, 23, 641-643.	4.1	115
169	A Phenotypic Small-Molecule Screen Identifies an Orphan Ligand-Receptor Pair that Regulates Neural Stem Cell Differentiation. Chemistry and Biology, 2007, 14, 1019-1030.	6.0	67
170	Epigenetic Regulation of Stem Cell Differentiation. Pediatric Research, 2006, 59, 21R-25R.	2.3	153
171	Neural progenitors populate the cerebrospinal fluid of preterm patients with hydrocephalus. Journal of Pediatrics, 2006, 148, 337-340.e3.	1.8	23
172	The Ups and Downs of BDNF in Rett Syndrome. Neuron, 2006, 49, 321-323.	8.1	39
173	Coupling of cell migration with neurogenesis by proneural bHLH factors. Proceedings of the National Academy of Sciences of the United States of America, 2006, 103, 1319-1324.	7.1	195
174	A positive autoregulatory loop of Jak-STAT signaling controls the onset of astrogliogenesis. Nature Neuroscience, 2005, 8, 616-625.	14.8	350
175	DNA methylation controls the timing of astrogliogenesis through regulation of JAK-STAT signaling. Development (Cambridge), 2005, 132, 3345-3356.	2.5	371
176	R/qtl: QTL mapping in experimental crosses. Bioinformatics, 2003, 19, 889-890.	4.1	3,197
177	DNA Methylation-Related Chromatin Remodeling in Activity-Dependent <i>Bdnf</i> Gene Regulation. Science, 2003, 302, 890-893.	12.6	1,315
178	MAANOVA: A Software Package for the Analysis of Spotted cDNA Microarray Experiments. Statistics in the Health Sciences, 2003, , 313-341.	0.2	165
179	Zfp281 Inhibits the Pluripotent-to-Totipotent State Transition in Mouse Embryonic Stem Cells. Frontiers in Cell and Developmental Biology, 0, 10, .	3.7	4